arXiv:cond-mat/0512147v1 [cond-mat.other] 7 Dec 2005

Structural transitions in the 309-atom magic number Lennard-Jones cluster

Eva G. Noya and Jonathan P. K. Doye
University Chemical Laboratory, Lensfield Road, Cambridge CB2 1EW, United Kingdom

(Dated: February 2, 2008)

The thermal behaviour of the 309-atom Lennard-Jones cluster, whose structure is a complete Mackay icosahedron, has been studied by parallel tempering Monte Carlo simulations. Surprisingly for a magic number cluster, the heat capacity shows a very pronounced peak before melting, which is attributed to several coincident structural transformation processes. The main transformation is somewhat akin to surface roughening, and involves a cooperative condensation of vacancies and adatoms that leads to the formation of pits and islands one or two layers thick on the Mackay icosahedron. The second transition in order of importance involves a whole scale transformation of the cluster structure, and leads to a diverse set of twinned structures that are assemblies of face-centred-cubic tetrahedra with 6 atoms along their edges, i.e., one atom more than the edges of the 20 tetrahedra that make up the 309-atom Mackay icosahedron. A surface reconstruction of the icosahedron from a Mackay to an anti-Mackay overlayer is also observed, but with a lower probability.

PACS numbers: 61.46.Bc,36.40.Ei,36.40.Mr

I. INTRODUCTION

Lennard-Jones (LJ) clusters have been widely studied over the last few decades and have become a model system for understanding some of the structural, thermodynamic and dynamic properties that are particular to clusters. This choice is mainly due to the simplicity of the model, but it also reflects the possibility of making comparisons with experiments on rare gas clusters. For example, the ground-state structure of all LJ clusters with up to 1600 atoms has now been investigated.[1,2,3,4,5,6,7,8,9,10,11,12,13] It is well-established that, for $N < 1000$, LJ clusters follow an icosahedral pattern growth, showing magic numbers corresponding to complete Mackay icosahedra at $N = 13$, 55, 147, 309, 561, and 923. In between these magic numbers, the vast majority of the global minima correspond to a Mackay icosahedron core covered by an incomplete outer layer. The exceptions occur at or near to shell closings of alternative structural forms. Mostly, these correspond to Marks decahedra, but there is also one instance of a face-centred-cubic (fcc) truncated octahedron ($N = 38$)[2,3] and of a Leary tetrahedron ($N = 98$).[9]

There are two different ways in which a layer can grow on the surface of a Mackay icosahedron, which are termed Mackay and anti-Mackay growth modes.[1] A Mackay icosahedron can be considered to be made up of twenty slightly distorted fcc tetrahedra sharing a common vertex. The Mackay growth mode continues the fcc packing of the underlying tetrahedra, leading to the next Mackay layer, whilst the anti-Mackay growth mode involves sites that are in hexagonal close packing positions with respect to the underlying tetrahedra, thus introducing a twin plane. The two overlayers are illustrated in Fig. 1. The growth of a new shell in LJ clusters usually starts at the anti-Mackay sites, as this overlayer does not involve low-coordinate edge atoms. However, as the Mackay overlayer is associated with a higher surface density, it has a lower strain energy and becomes energetically favourable over the anti-Mackay above a given size.

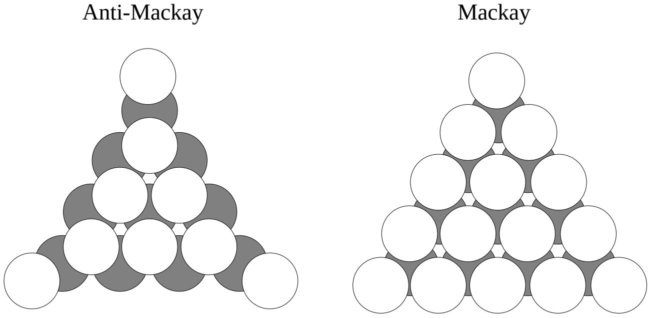

FIG. 1: Atomic positions for the two possible overlayers on a 147-atom Mackay icosahedron.

The thermal behaviour of LJ clusters has also been much studied.[14,15,16,17,18,19,20,21,22,23,24,25,26,27,28,29,30] It is known that many clusters do not retain the ground-state structure up to melting, but, instead, they undergo structural changes as the temperature is raised. For LJ clusters, solid-solid transitions prior to melting can be expected for those sizes with non icosahedral geometries.[19,20,21,25,26,27,28,30] Premelting effects associated with structural changes at the surface that lead to enhanced surface diffusion are also common.[16,18] Of particular interest to us here are the surface reconstructions which can occur for clusters with an incomplete Mackay overlayer and in which the outer layer changes from Mackay to anti-Mackay.[24,29] This surface reconstruction is mainly driven by the greater vibrational entropy associated with anti-Mackay structures. For a particular shell, the transition is first seen at the crossover size at which a Mackay structure becomes lowest in energy (e.g. at $N = 31$ for the second shell, and at $N = 82$ for the third shell), and also occurs at the subsequent sizes but at a temperature that increases with the cluster's size. Therefore, there comes a size for which the melting temperature becomes lower than the temperature necessary for the surface reconstruction to occur and, so, the surface reconstruction only takes place in a limited size range, namely $N = 31 - 39$[23,24,29] for the second Mackay layer and $N = 82 - 140$[29] for the third Mackay layer.

As the growth of the fourth shell of the Mackay icosahedron follows the same pattern as the previous ones, it is very likely that the surface reconstruction again occurs. The results for the second and third layer seem to indicate that there might be a tendency for the size range over which the surface reconstruction takes place to increase with the number of shells. In particular, if the upper size for which this transition occurs continues to increase with the shell number, it might be that even the complete 309-atom Mackay icosahedron could undergo such a surface reconstruction as well. This would be an unexpected result, since usually magic numbers clusters will show a single 'first-order-like' melting peak in the heat capacity, and 'premelting' and other transitions are more generally associated with incomplete shells. Indeed, Labastie and Whetten's classical paper on the size evolution of cluster melting towards the bulk first-order behaviour, was based on the Mackay icosahedral LJ clusters with 13, 55 and 147 atoms.[15] However, there is some precedent for such a transition in a complete Mackay icosahedron. For Morse clusters, it has already been shown that such a surface reconstruction occurs prior to melting for $N =$ 561 and 923,[31] although the parameter in the Morse potential that determines the range of the potential had a value for which anti-Mackay structures are stabilized relative to the LJ potential.[32] Therefore, a study of the melting behaviour of the 309-atom LJ cluster would serve both to test our hypothesis concerning a possible surface reconstruction and to better understand the thermodynamics of surface transitions in clusters.

II. METHODS

The potential energy of a cluster interacting with the LJ potential is given by

$$E = 4\epsilon \sum_{i<j} \left[\left(\frac{\sigma}{r_{ij}} \right)^{12} - \left(\frac{\sigma}{r_{ij}} \right)^{6} \right], \qquad (1)$$

where ϵ is the pair well depth and $2^{1/6}\sigma$ is the equilibrium pair separation.

The thermal behaviour of the LJ 309-atom complete Mackay icosahedron was studied using canonical Monte Carlo (MC) simulations with the parallel tempering exchange scheme (PT).[33] The PT MC simulations consisted of 32 trajectories at temperatures ranging from $0.360\,\epsilon/k_B$ to $0.453\,\epsilon/k_B$. A preliminary study over a broader range of temperatures, from $0.010\,\epsilon/k_B$ to $0.600\,\epsilon/k_B$, showed that the region $0.360\,\epsilon/k_B$ - $0.453\,\epsilon/k_B$ was wide enough to capture all the interesting features of the heat capacity curve. Due to the slow convergence, the system was equilibrated by performing $7.2\ \times 10^7$ MC cycles for each one of the trajectories, and the data to compute the heat capacity were collected over the following 3.06×10^8 MC cycles. Similar convergence problems have already been encountered in previous PT MC studies of the thermal behaviour of smaller LJ clusters.[20,21,26,27,28,29] Exchanges between two trajectories were attempted with a probability of 10%. All the temperatures were initialized with the Mackay icosahedron ground-state structure. Evaporation and fragmentation of the cluster was avoided by adding a hard wall of radius $r + \sigma$, where r is the radius of the ground-state structure. The heat capacity and caloric curves were obtained from the simulation data using the multihistogram technique.[15]

III. RESULTS

In Fig. 2 we have plotted the canonical and microcanonical caloric curves and the canonical heat capacity, as obtained from our simulations using the multihistogram technique. There are two fairly sharp changes in the slope of the canonical caloric curve, which, in the microcanonical ensemble, lead to two van der Waals loops, i.e. regions in which the caloric curve exhibits a negative slope and the heat capacity is negative. Coincident with these features in the caloric curves, at the temperatures $0.390\,\epsilon/k_B$ and $0.417\,\epsilon/k_B$, the canonical heat capacity curve shows two clearly distinct peaks. The height of the first peak is roughly half the height of the second one, but the former is slightly broader. The latent heat of these transitions was computed as the area under each peak in the heat capacity curve. It was found that the latent heat associated with the first peak is approximately $0.67\,l_m$, where $l_m = 0.29/N\epsilon$ is the latent heat of the second peak, which, as we will show below, signals the melting of the cluster. These results indicate that the 309-atom LJ cluster undergoes a major structural transition before melting. The unusual presence of two van der Waals loops in the microcanocial caloric curve, as well as the two strong peaks in the canonical heat capacity, suggest that this transition might be, as with the cluster melting transition, the finite-size analogue of a first-order transition.[15] In the regions where the microcanonical heat capacity is negative, the canonical probability distribution for the energy is also bimodal.[34]

The structural transformations associated with the two peaks in the heat capacity curve were analyzed by performing systematic quenches starting from configurations generated in each of the 32 trajectories employed in our calculations.[35] Two useful properties to characterize the minima are their potential energy and geometric mean vibrational frequency $\bar{\nu}$. The main contributions to $\bar{\nu}$ come from atoms which are nearest neighbours. For a pair potential, such as LJ, the value of $\bar{\nu}$ reflects both the number of nearest neighbours, and the average nearest-neighbour distance, the latter because the

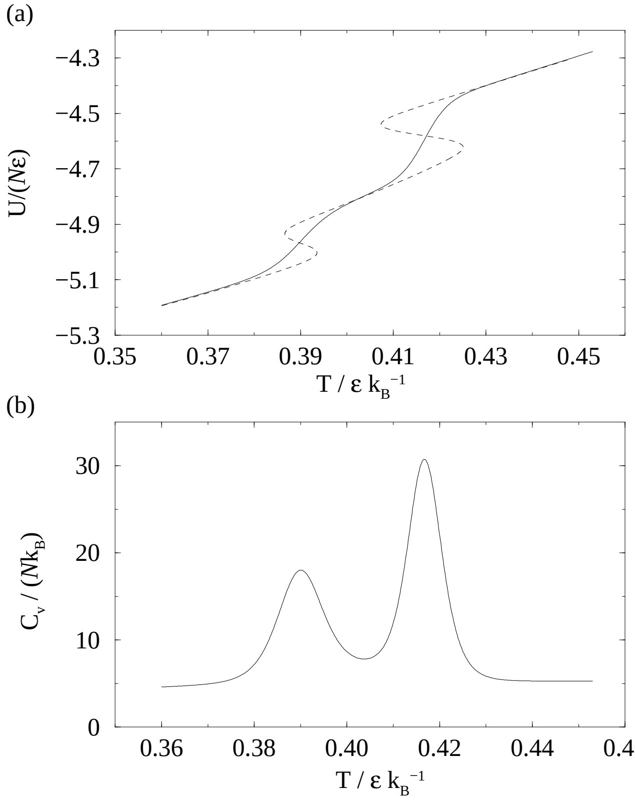

FIG. 2: (a) Canonical (solid line) and microcanonical (dashed line) caloric curves and (b) canonical heat capacity for the 309-atom LJ cluster.

second derivative of the LJ potential decreases with distance. Strained structures, which inevitably have a variety of nearest-neighbour distances, have a larger average nearest-neighbour distance, because of the anharmonic nature of the LJ well, and hence have smaller values of $\bar{\nu}$.

Plotting $\bar{\nu}$ against the potential energy for the minima we obtained shows that they can be naturally divided into a number of types, which, as we will see, reflect their different structural features (see Fig. 3(a)). Specifically, the diagram can be divided into four well-defined zones, with only a relatively small number of minima near to the boundaries. A closer inspection of zone 2 shows that this zone can be further divided into two subzones (2A and 2B) on the basis of their frequencies, but the division in this case is less clear cut.

To determine the structural types associated with the different zones in Fig. 3(a) we visually inspected a large number of minima. To facilitate this task, we also performed common neighbour analyses of the structures,[36,37,38] and so we were able to identify atoms that had a particular local coordination environment. It was particularly noteworthy that all the minima in zones 1, 2 and 3 are ordered in the sense that all the atoms in the interior of these clusters have twelve nearest neighbours, whose local coordination shell can be characterized as icosahedral, decahedral, fcc or hcp.[38] Typical isomers representative of each zone are depicted in Fig. 4.

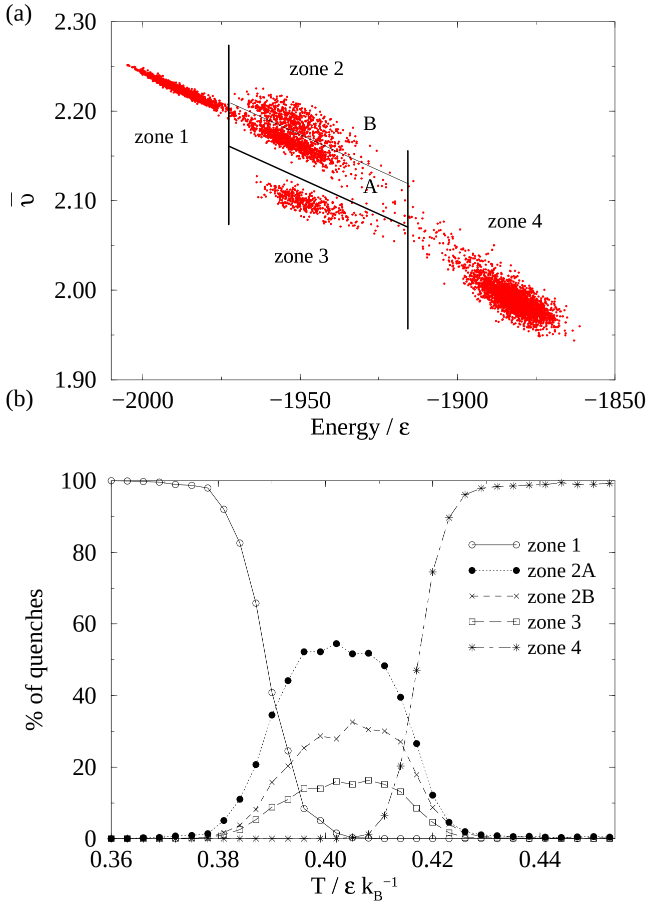

FIG. 3: (a) (Colour online) A scatter plot of the geometric mean vibrational frequency against the potential energy for the minima collected from the quenches at all temperatures. Five distinct zones can be distinguished in this diagram, and the boundaries that we have chosen to delineate these zones are explicitly shown in the plot. The unit of frequency is $(\epsilon/m\sigma^2)^{(1/2)}$. (b) The percentage of quenches that lead to minima in each of the five zones as a function of temperature.

The lowest energy region (Energy $< -1972\,\epsilon$), designated as zone 1, corresponds to the global minimum, the complete Mackay icosahedron, and structures based upon it, in which there are some vacancies at the low-coordinate vertex and edge sites, and the resulting adatoms are dispersed across the surface of the cluster, perhaps forming adatom clusters of a few atoms (see structure (1) in Fig. 4). As the number of vacancies increases, the potential energy of the minima increases, and their mean vibrational frequency decreases due to the lowered number of nearest neighbours.

At energies in the interval $-1972\,\epsilon$ to $-1915\,\epsilon$, there are two clearly separate regions differentiated by their vibrational frequency. As mentioned above, the higher frequency region, zone 2, is further divided into two subzones designated as 2A and 2B. The isomers found in zone 2A are Mackay icosahedra in which a pit is formed on one side of the cluster, whilst an adatom island is formed on the opposite side (see structures (2A) I and II in Fig. 4). The islands prefer to occupy anti-Mackay sites, and both the pits and islands can be one or two layers thick. These structures are therefore similar to those of zone 1, but have a significantly larger density of adatoms and vacancies. Consistent with this, the zone 2A minima form a downwardly sloping band in Fig. 3(a), that can be seen to be an extension of the band due to the zone 1 minima. However, there is a clear gap between these two bands at the boundaries between zones 1 and 2A, because minima with an intermediate number of surface defects are less likely to be sampled.

It used to be common to refer to a Mackay icosahedron as a multiply-twinned particle,[39] because they are made of twenty somewhat strained fcc tetrahedra sharing a common vertex. The twin planes correspond to the internal faces of these tetrahedra and which are common to two tetrahedra. For the 309-atom Mackay icosahedron there are five atoms along the edges of the fcc tetrahedra. Other multiply twinned structures that are also made up of aggregates of fcc tetrahedra are possible, such as the Marks decahedra[40] and the Leary tetrahedron.[9]

After an extensive investigation of the structures of the minima in zone 2B, in which the common neighbour analysis was particularly revealing, we found that the common feature of this diverse set of structures was that they are aggregates of fcc tetrahedra with 6 atoms per edge. As the fcc tetrahedra are larger than for structures based on the 309-atom Mackay icosahedron, the structures are less strained, and so have larger vibrational frequencies. Three different examples of the possible arrangements of the fcc tetrahedra are shown in Fig. 4. For structure (2B) I there is a single complete fcc tetrahedron at the centre of the cluster and it is related to a Leary tetrahedron.[9] Structure (2B) II has two twinned fcc tetrahedra at its centre. Finally, structure (2B) III has five fcc tetrahedra (some incomplete) sharing a common edge, and so it has a decahedral structure at its core. In all these structures, these central tetrahedra are covered by overlayers that begin the growth of new tetrahedra that are twinned with respect to the core.

The lowest vibrational frequency region at intermediate energies, zone 3, is occupied by isomers with a 147-atom Mackay icosahedral core, but where the outer layer has undergone a surface reconstruction from a Mackay to an anti-Mackay overlayer. Because of the greater strain associated with these structures, they have a lower mean vibrational frequency. As mentioned in the introduction, a similar surface reconstruction has been observed for some smaller LJ clusters with incomplete Mackay layers[24,29] and for larger complete Mackay icosahedra interacting with a long-ranged Morse potential.[31] As seen in Fig. 3 (a), this surface reconstruction is partly driven by the higher vibrational entropy of the anti-Mackay overlayer. In addition, covering the 147-atom Mackay icosahedron with a complete anti-Mackay overlayer gives rise to a 279-atom structure, and so there is also a configurational entropy gain associated with the possible arrangements of the 30 extra adatoms.

Note that the edges of the underlying fcc tetrahedra around which the above anti-Mackay structures are formed have only four atoms along their edges. Therefore, we can conclude that the three regions at intermediate energies correspond to structures built around assemblies of fcc tetrahedra, but, depending on the length of the edges of these tetrahedra, and hence the associated strain, the isomers fall in different regions of frequency.

Finally, the high energy region, zone 4, is associated with completely melted structures, in which both the core and surface atoms are disordered. There is a variety of coordination numbers associated with the interior atoms in these structures. Furthermore, the common neighbour analysis shows that the vast majority of the atoms do not have an ordered local coordination shell. Therefore, zone 4 is assigned to the liquid state.

An analysis of the quench results is presented in Fig. 3 (b) showing the percentage of quenches that lead to minima in the different zones. At temperatures below that for the first peak almost all isomers found correspond to Mackay icosahedra in which a number of vacancies and adatoms are formed on the cluster's surface. The vacancies mainly appear at the low-coordinate vertex and edge sites, whilst the adatoms diffuse around the surface, as seen previously for smaller Mackay icosahedra.[16,41] At temperatures coincident with the first peak there is a fairly sharp transition from the Mackay icosahedron with a small number of defects to structures which have undergone some kind of structural transition. Surprisingly, the Mackay to anti-Mackay reconstruction represents only a minor contribution to the heat capacity, with only up to around a 15-20% probability of finding the cluster with an anti-Mackay reconstructed surface. Instead, two other transitions dominate in this range of temperatures.

In the main transition, which represents a 50-55% of the total transition, adjacent atoms from the outer shells of the Mackay icosahedron vacate their sites, leaving behind pits one or two layers thick, and the resulting adatoms form islands above the still intact parts of the fourth shell. As mentioned above, below the transition, the vacancies and adatoms associated with the Mackay icosahedron are dispersed across the surface and their number gradually increases with temperature. However, as the surface density of these defects increases there comes a point where there is a jump in the number of vacancies and adatoms, and they cluster together to form islands and pits. This process is driven by the (effective) attraction between the adatoms and vacancies. Once a number of vacancies are formed at vertex and edge sites, the neighbouring atoms also lower their coordination number and, therefore, it becomes more favourable to remove more vertex and face atoms in positions adjacent to an already existing vacancy or pit. This transition is somewhat akin to the pre-roughening and roughening

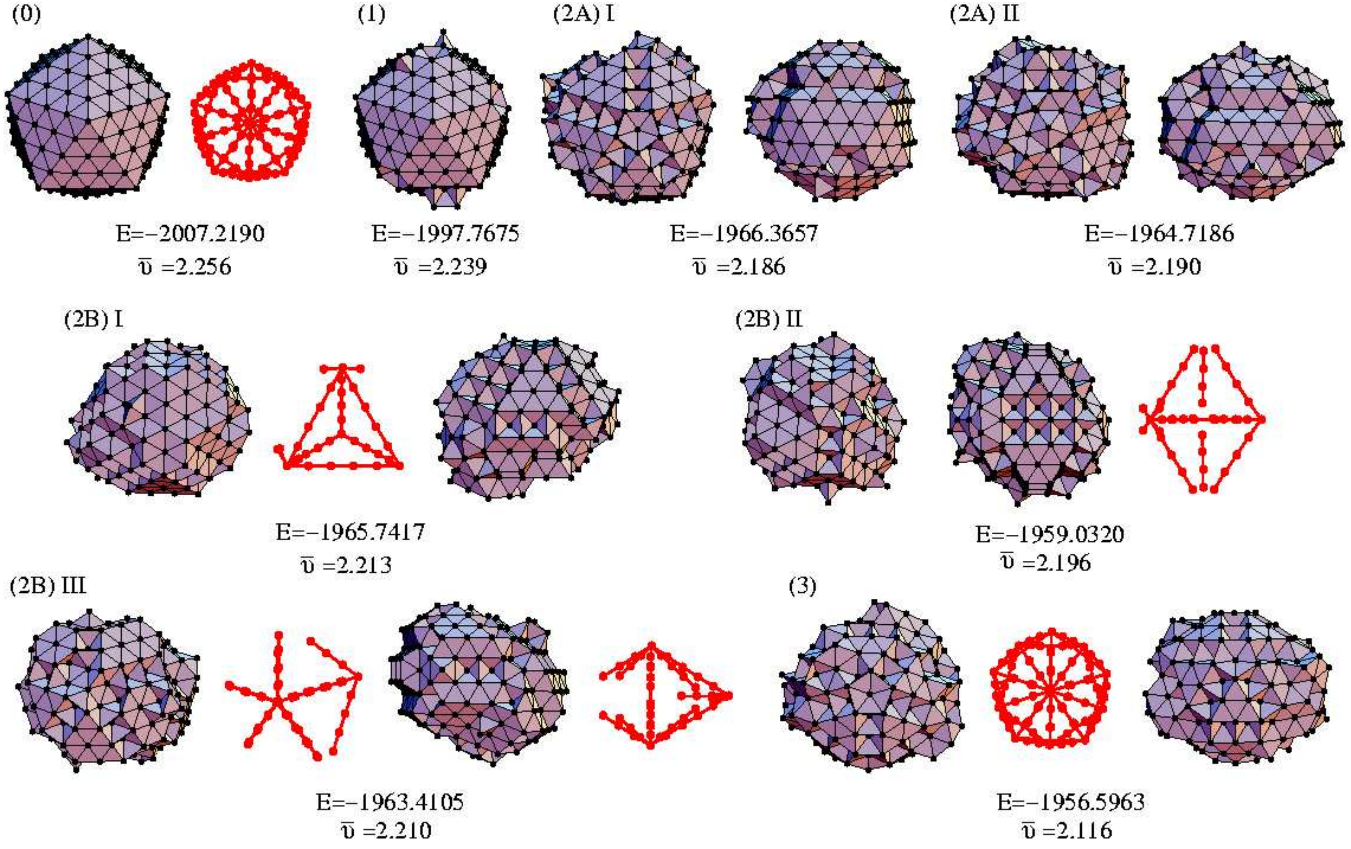

FIG. 4: (Colour online) Structure of the global minimum and of some of the isomers representative of the zones shown in Fig. 3(a). The energy and frequency are given in reduced units. To illustrate how the structures can be viewed as assemblies of fcc tetrahedra, to the right of some of the complete structures, we have also depicted the network formed by those atoms that lie along the edges of these tetrahedra.

transtions,[42] both of which are known to occur for the bulk LJ {111} surfaces.[43,44]

The second transition competing with the Mackay to anti-Mackay surface reconstruction, is not a surface transition, but involves a transformation of the whole structure of the cluster. The resulting structures are multiply-twinned particles that are assemblies of fcc tetrahedra with six atoms along each edge, one atom more than the tetrahedra that make up the 309-atom Mackay icosahedron. This transition must be driven by an increase in the configurational entropy, as these structures have lower vibrational entropies. Indeed, this conformational entropy is reflected in the diversity of structures that we observed (Fig. 4). The probability that these structures are adopted reaches a maximum of about 30% midway between the two heat capacity peaks.

Finally, as the second heat capacity peak is approached and the cluster begins to melt, this array of different structures becomes less probable in favour of disordered structures typical of the liquid state.

IV. CONCLUSIONS

The existence of a well-defined structural transition in the 309-atom LJ cluster prior to melting suggests that, as we anticipated in the introduction of this paper, there is a tendency for the size range for which LJ clusters with Mackay overlayers undergo structural transformations prior to melting to increase as the number of shells in the cluster increases. For the fourth icosahedral shell, we expect these transitions to begin at around $N = 169$, the size at which a Mackay overlayer becomes energetically more favourable than the anti-Mackay, and to continue up to, and probably beyond, the next complete Mackay icosahedron at $N = 309$. This compares to $N = 31 - 39$ and $N = 82 - 140$ for the second and third icosahedral shells. However, the unexpected aspect of our results was the nature of the transition that occurred and the size of the heat capacity peak that resulted. Contrary to our predictions, the Mackay to anti-Mackay surface reconstruction was only a minor contribution to the heat capacity peak. Instead, two other transitions had a more significant effect. In particular, the dominant contribution is from a surface transition involving the condensation of vacancies and adatoms that leads to the formation of pits and islands one or two layers thick on the Mackay icosahedron. Also fairly important was another transition that leads to a complete loss of the Mackay icosahedral structure, and the adoption of multiply-twinned structures based upon packings of fcc tetrahedra with six atoms along each edge. By contrast, the twenty strained fcc tetrahedra that make up the 309-atom Mackay icosahedron have five atoms along each edge.

The substantial latent heat, the van der Waals loop in the microcanonical caloric curve, and the bimodal distribution for the energy in the canonical ensemble, all suggest that the transition at T=$0.390\,\epsilon/k_B$ is the finite size analogue of a first order phase transition. But does it have any analogues in bulk systems? The two more minor transitions that contribute to the peak clearly have no bulk analogue, as they are specific to Mackay icosahedra and multiply-twinned particles, both of which will not be energetically competitive in the bulk limit. However, as we have already mentioned, the cooperative condensation of the vacancies and adatoms to form pits and islands, respectively, has some similarities to the bulk pre-roughening and roughening transitions[42] of the LJ fcc {111} surfaces.[43,44] All involve the loss of the uniform, flat character of the perfect {111} surfaces through the formation of islands and pits, whilst retaining the basic lattice structure. However, the pre-roughening transition leads to a disordered flat surface, where the height fluctuations are restricted to be of one layer thickness, whereas, for the clusters, islands and pits are seen that can be two layers high or deep. The surface roughening transition is defined as the temperature at which a height-height correlation function diverges with distance. However, such a definition cannot be straightforwardly applied to our cluster, because the {111} facets are so small. Furthermore, the cooperative nature of the transition is also related to the small size of the facets, since it allows the removal of whole faces, nucleated by the preferential generation of vacancies at the vertices and edges. Therefore, it would premature to say that the transition in our clusters *is* the finite size analogue of either the pre-roughening or roughening transitions, and it would be interesting to see how the transition evolves with cluster size.

Our results have also shown that even for a very strong magic number, such as the 309-atom LJ cluster, the heat capacity curve can exhibit strong features prior to melting. This is an important finding, because usually it is expected that magic numbers will show only one well-defined melting peak in the heat capacity curve, whilst premelting effects and other structural transitions are more generally associated with clusters with incomplete shells. For example, following the scaling arguments of Labastie and Whetten, which were based on the first three LJ Mackay icosahedra,[15] it would have been expected that the 309-atom cluster would exhibit a single heat capacity peak that was narrower and higher than for the 147-atom cluster, hence smoothly converging towards the bulk limit. Our results have shown that this an oversimplified view of the problem and that many surprising features can appear along the path towards the bulk limit. Indeed, one should expect structural transitions prior to melting to be the norm for larger LJ clusters up to very large sizes. Firstly, larger Mackay icosahedra would be expected to show similar transitions to those found here. Secondly, even at sizes when decahedral and then fcc structures become lowest in energy, there are likely to be solid-solid transitions from decahedral to icosahedral and at larger sizes from fcc to decahedral, driven by differences in vibrational entropy.[25]

Acknowledgments

The authors are grateful to the Ramón Areces Foundation (E.G.N.) and the Royal Society (J.P.K.D.) for financial support, and to Florent Calvo for helpful discussions.

---

[1] J. A. Northby, J. Chem. Phys. **87**, 6166 (1987).

[2] J. Pillardy and L. Piela, J. Phys. Chem. **99**, 11805 (1995).

[3] J. P. K. Doye, D. J. Wales, and R. S. Berry, J. Chem. Phys. **103**, 4234 (1995).

[4] J. P. K. Doye and D. J. Wales, Chem. Phys. Lett. **247**, 339 (1995).

[5] D. M. Deaven, N. Tit, J. R. Morris, and K. M. Ho, Chem. Phys. Lett. **10**, 25 (1996).

[6] D. J. Wales and J. P. K. Doye, J. Phys. Chem. A **101**, 5111 (1997).

[7] D. Romero, C. Barrón, and S. Gómez, Comp. Phys. Comm. **123**, 87 (1999).

[8] B. Hartke, J. Comp. Chem. **20**, 1752 (1999).

[9] R. H. Leary and J. P. K. Doye, Phys. Rev. E **60**, R6320 (1999).

[10] Y. H. Xiang, H. Y. Jiang, W. S. Cai, and X. G. Shao, J. Phys. Chem. A **108**, 3586 (2004).

[11] Y. H. Xiang, L. J. Cheng, W. S. Cai, and X. G. Shao, J. Phys. Chem. A **108**, 9516 (2004).

[12] X. G. Shao, Y. H. Xiang, and W. S. Cai, J. Phys. Chem. A **109**, 5193 (2005).

[13] An up-to-date list of the Lennard-Jones global minima for $N \leq 150$ and $310 \leq N \leq 1000$ can be found at The Cambridge Cluster Database, http://www-wales.ch.cam.ac.uk/CCD.html.

[14] R. S. Berry, T. L. Beck, H. L. Davis, and J. Jellinek, Adv. Chem. Phys. **70**, 75 (1988).

[15] P. Labastie and R. L. Whetten, Phys. Rev. Lett. **65**, 1567 (1990).

[16] H.-P. Cheng and R. S. Berry, Phys. Rev. A **45**, 7969 (1992).

[17] D. D. Frantz, J. Chem. Phys. **102**, 3747 (1995).

[18] F. Calvo and P. Labastie, Chem. Phys. Lett. **109**, 233 (1996).

[19] J. P. K. Doye, D. J. Wales, and M. A. Miller, J. Chem.

Phys. **109**, 8143 (1998).

[20] J. P. Neirotti, F. Calvo, D. L. Freeman, and J. D. Doll, J. Chem. Phys. **112**, 10340 (2000).

[21] F. Calvo, J. P. Neirotti, D. L. Freeman, and J. D. Doll, J. Chem. Phys. **112**, 10350 (2000).

[22] F. Calvo, J. P. K. Doye, and D. J. Wales, J. Chem. Phys. **114**, 7312 (2001).

[23] D. D. Frantz, J. Chem. Phys. **115**, 6136 (2001).

[24] F. Calvo and J. P. K. Doye, Phys. Rev. E **63**, 010902 (2001).

[25] J. P. K. Doye and F. Calvo, J. Chem. Phys. **116**, 8307 (2002).

[26] D. Sabo, D. L. Freeman, and J. D. Doll, J. Chem. Phys. **122**, 094716 (2005).

[27] C. Predescu, P. A. Frantsuzov, and V. A. Mandelshtam, J. Chem. Phys. **122**, 154305 (2005).

[28] H. Liu and K. D. Jordan, J. Phys. Chem. A **109**, 5203 (2005).

[29] P. A. Frantsuzov and V. A. Mandelshtam, Phys. Rev. E **72**, 037102 (2005).

[30] V. A. Mandelshtam, A. Frantsuzov, and F. Calvo, submitted.

[31] J. P. K. Doye and D. J. Wales, Z. Phys. D: At., Mol. Clusters **40**, 466 (1997).

[32] J. P. K. Doye and D. J. Wales, J. Chem. Soc., Faraday Trans. **93**, 4233 (1997).

[33] R. H. Swendsen and J.-S. Wang, Phys. Rev. Lett. **57**, 2607 (1986).

[34] D. J. Wales and R. S. Berry, Phys. Rev. Lett. **73**, 2875 (1994).

[35] D. J. Wales and R. S. Berry, J. Chem. Phys. **92**, 4283 (1990).

[36] H. Jonsson and H. C. Andersen, Phys. Rev. Lett. **60**, 2295 (1988).

[37] A. S. Clarke and H. Jonsson, Phys. Rev. E **47**, 3975 (1993).

[38] S. C. Hendy and B. D. Hall, Phys. Rev. B **64**, 085425 (2001).

[39] A. Howie and L. D. Marks, Philos. Mag. A **49**, 95 (1984).

[40] L. D. Marks, Philos. Mag. A **49**, 81 (1984).

[41] R. E. Kunz and R. S. Berry, Phys. Rev. Lett. **71**, 3987 (1993).

[42] J. D. Weeks, in *Ordering in Strongly Fluctuating Condensed Matter Systems*, edited by T. Riste (Plenun, New York, 1980), p. 293.

[43] F. Celestini, D. Passerone, F. Ercolessi, and E. Tosatti, Surf. Sci. **402**, 886 (1998).

[44] U. Tartaglino, T. Zykova-Timan, F. Ercolessi, and E. Tosatti, Phys. Rep. **411**, 291 (2005).